ZIBELINE INTERNATIONAL™ PUBLISHING

ISSN: 2521-5051 (Print)
ISSN: 2521-506X (Online)
CODEN: ASMCCQ

Acta Scientifica Malaysia (ASM)

DOI: http://doi.org/10.26480/asm.01.2021.27.35

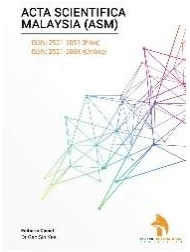

RESEARCH ARTICLE

ADSORPTIVE REMOVAL OF METHYLENE BLUE FROM SYNTHETIC WASTEWATER USING DATE PALM SEEDS, GOETHITE AND THEIR COMPOSITE

Nasir Abdus-Salam, Abiola Victoria Ikudayisi-Ugbe*, Fabian Audu Ugbe

Department of Chemistry, Faculty of Physical Sciences, University of Ilorin, P.M.B. 1515, Ilorin, Nigeria.
Corresponding Author Email: ikudayisiabiola@gmail.com

ARTICLE DETAILS

Article History:

Received 10 January 2021
Accepted 16 February 2021
Available online 05 April 2021

ABSTRACT

The adsorption of Methylene Blue (MB) onto Raw Date-palm Seeds (RDS), Thermally Activated Carbon (TAC), Chemically Activated Carbon (CAC), Goethite (GT) and their Composite (COM) were studied using batch equilibrium technique. Variations of sorptive properties such as initial solution concentration, pH, adsorbent dosage, contact time and temperature had a remarkable influence on the adsorption processes. The data fitted well tested isotherm models in the order; Langmuir (R^2 = 0.942 and 0.963) > Freundlich (0.886 and 0.948) > Temkin (0.869 and 0.83) for GT and COM respectively. That of CAC and TAC was best described by Freundlich and Langmuir models respectively while RDS showed very poor fittings. Pseudo-second order and film diffusion models best described the adsorption kinetics. The adsorption was feasible, spontaneous ($\Delta G < 0$) and exothermic (except MB-CAC with ΔH being positive). The combined results of isotherm, kinetics and thermodynamic studies suggested a combined chemisorptions and physisorptions processes. Also, the kinetic modeling suggested that intra-particle and film diffusions occurred simultaneously and/or in combination with other processes in the mechanism of adsorption.

KEYWORDS

Adsorption, date palm seeds, methylene blue, isotherm, kinetics.

1. INTRODUCTION

Environmental pollution has become increasingly prominent with continuous growth in technology across the globe (Luo et al., 2019). The discharge of dye effluents from industries such as textiles, leather, food, polymers, pharmaceutical, and cosmetics into the water system constitutes a major concern due to the adverse effects on human and aquatic lives (Zargar et al., 2011; Elmorsi et al., 2019). Some health complications associated with ingestion of dye polluted water include shock, diarrhea, jaundice, allergies, skin irritation, or different tissue changes etc. (Luo et al., 2019; Saini, 2017).

Treatment of dye effluents constitutes a significant environmental issue because synthetic dyes are known to have complex aromatic structures which offer them inertness and non-biodegradability (Zargar et al., 2011; Mohamed and Ahmed, 2017; Funtua and Ugbe, 2015). However, many techniques such as advanced oxidation, flocculation, biodegradation, photo-degradation, electrodialysis, membrane filtration, and adsorption have been developed and applied in the treatment of dye effluents (Sajab et al., 2011; Arunachalam et al., 2018; Ansari and Mosayebzadeh, 2010; Elmorsi, 2011; Ardalan, 2014). Adsorption is one of the most popular methods amongst these because of their low cost, high efficiency and ease of handling (Anirudhan and Rejeena, 2015).

The date palm (*Phoenixdactylifera*), a tropical and subtropical tree that is now much available mostly in the North-west and North-eastern parts of Nigeria can be traced back to the Middle East and North Africa where it was sourced (Abdullahi et al., 2015; Chandrasekaran and Bahkali, 2012). Experiment showed that date seeds contain approximately 55-65 % of carbohydrates, an indication that activated carbon of high-grade can be obtained due to their high carbon content (Arshad et al., 2014). On the other hand, synthetic goethite when compared with their naturally occurring counterparts has an improved purity and tailored composition with desired surface properties and particle size (Nayak and Rao, 2005). Generally, goethite (FeO(OH)) contains the hydroxyl group which makes it easier to bind strongly to both organic and inorganic ligands (Liu and Chen, 2013). It equally shows high specific surface areas and strong affinities for surface binding (Wang et al., 2019).

In search of low-cost adsorbents, some researchers earlier investigated the adsorption properties of locally available materials such as Biochar, raw and roasted date seed, tea waste carbon, termite mound and goethite amongst others (Zhanga et al., 2020; Marouani et al., 2018; Borah et al., 2015; Anebi et al., 2016; Ugbe and Abdus-Salam, 2020; Abdus-Salam et al., 2020). Therefore, the adsorptive properties of date palm seeds, goethite and their composite for MB (Figure 1) were investigated to provide insights into the optimum operating conditions, feasibility and possible mechanism of fixation of this dye onto the various adsorbents surfaces.

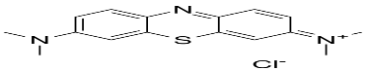

Figure 1: Chemical structure of Methylene Blue

Quick Response Code	Access this article online	
	Website: www.actascientificamalaysia.com	**DOI:** 10.26480/asm.01.2021.27.35

Cite the Article: Nasir Abdus-Salam, Abiola Victoria Ikudayisi-Ugbe, Fabian Audu Ugbe (2021). Adsorptive Removal of Methylene Blue from Synthetic Wastewater Using Date Palm Seeds, Goethite and Their Composite. *Acta Scientifica Malaysia, 5(1): 27-35.*

2. Material and Methods

2.1 Preparation of the Adsorbents

All the adsorbents used in this study were prepared according to the procedures and methods earlier described (Abdus-Salam and Ikudayisi, 2017).

2.2 Adsorbate Preparation and Calibration Curve

The adsorbate, MB was purchased from Sigma Aldrich and used in this study without further purification. A 1.0 g MB was weighed into a 1000ml capacity volumetric flask, dissolved and made up to mark with deionized water to make 1000 mg/L from which other lower working concentrations (2, 4, 6, 8 and 10 mg/L) were prepared by the method of serial dilution. The absorbances of the various solutions were determined using the UV-Visible spectrophotometer at a wavelength of 668 nm (Utsev et al., 2020). A plot of absorbance against concentration referred to as the calibration curve was then obtained.

2.3 Adsorption Experiment

Batch mode adsorption studies for methylene blue (MB) were carried out to investigate the effect of different parameters such as adsorbate concentration, adsorbent dosage, pH, temperature and contact time on date palm seeds (RDS, TAC and CAC), GT and composite of TAC and GT (COM). A 20 ml each of different concentrations; 25, 50, 75, 100, 125, 150, 175 and 200 mg/L MB were measured into separate 100 ml capacity conical flasks containing 0.2g RDS and agitated on an orbital mechanical shaker for 2 hrs. The solutions were then filtered and the resulting filtrates were analyzed using a UV-Visible spectrophotometer at a predetermined wavelength of maximum absorption (λ_{max}) of 668nm.

The procedure was repeated for 0.2g each of the TAC and CAC. For GT and COM, 15ml each of different concentrations; 10, 50, 100, 150, 200, 250, 300 and 400 mg/L MB were contacted with 0.1g each of both adsorbents. The optimum concentrations of MB obtained for the various adsorbents were then selected for use in the subsequent experiments. Further experiments were conducted using the optimum concentrations to examine the effects of variation of initial solution pH (2, 4, 6, 7, 8, 10 and 12), adsorbent dose (0.05, 0.1, 0.2, 0.3, 0.4 and 0.50 g), contact time (5, 10, 20, 30, 45, 60, 90 and 120 min) and temperature (25, 30, 40, 50, 60, 70 and 80 ºC).

The amounts of dye adsorbed at equilibrium were determined using equation 1 (Ugbe and Abdus-Salam, 2020).

$$q_e = \frac{V(C_i - C_e)}{m} \quad (1)$$

where,

q_e = dye amount (mg/g) taken by the adsorbent at equilibrium;
v = volume of dye solution (L);
C_i = initial dye concentration (mg/L);
C_e = equilibrium dye concentration (mg/L);
M = mass of adsorbent (g).

The experimental results were modeled using some selected isotherm models (Langmuir, Freundlich and Temkin), kinetic models (pseudo-first-order, pseudo-second-order, intra-particle diffusion and film diffusion), while some basic thermodynamic parameters such as Gibb's free energy change (ΔG), enthalpy change (ΔH) and entropy change (ΔS) were evaluated. The various equations with their parameters are presented in Table 1.

Table 1: Some adsorption isotherm, kinetics and thermodynamic equations and their parameters

Model	Equation	Linear plot	Eqn.	Author(s)
Langmuir	$\frac{C_e}{q_e} = \frac{1}{q_m}C_e + \frac{1}{K_a q_m}$ (a) $R_L = \frac{1}{1+K_a C_O}$ (b)	C_e/q_e vs C_e Slope: $1/q_m$ Intercept: $1/K_a q_m$	2	(Langmuir, 1916)
Freundlich	$logq_e = logK_F + \frac{1}{n}logC_e$	$\log q_e$ vs $\log C_e$ Slope: 1/n Intercept: $\log K_F$	3	(Freunlich, 1906)
Temkin	$q_e = BlnA + BlnC_e$ (a) $B = \frac{RT}{b}$ (b)	q_e vs lnC_e Slope: B Intercept: $BlnA$	4	(Temkin and Pyozhev, 1940)
Pseudo-first order	$\ln(q_e - q_t) = \ln q_e - k_1 t$	$\ln(q_e - q_t)$ vs t Slope: $-k_1$ Intercept: lnq_e	2	(Lagergren, 1989)
Pseudo- second order	$\frac{t}{q_t} = \frac{1}{k_2 q_e^2} + \left(\frac{1}{q_e}\right)t$	t/q_t vs t Slope: $1/q_e$ Intercept: $1/k_2 q_e^2$	3	(Ho and McKay, 1999)
Intra-particle diffusion	$q_t = k_{id} t^{\frac{1}{2}} + C$	q_t vs $t^{1/2}$ Slope: k_{id} Intercept: C	6	(Weber and Morris, 1963)
Film diffusion	$\ln\left[1 - \frac{q_t}{q_e}\right] = -R^1 t + C$ $R^1 = \frac{3D_e^1}{r_0 \Delta r_0 K'}$	$\ln\left[1 - \frac{q_t}{q_e}\right]$ vs t Slope: $-R^1$ Intercept: C	7	(Boyd et al., 1947)
Van't Hoff	$lnK_C = \frac{\Delta S}{R} - \frac{\Delta H}{RT}$ $K_C = \frac{C_S}{C_e}$ $\Delta G = \Delta H - T\Delta S$	$ln\,K_c$ vs 1/T Slope: $-\Delta H/R$ Intercept: $\Delta S/R$	8	(Ugbe et al., 2014; Al-Anber, 2011)

Isotherms

q_e = ads capacity ($mg.g^{-1}$)
q_m = monolayer ads capacity ($mg.g^{-1}$)
C_e = equil conc (mgL^{-1})
C_o = Initial conc (mgL^{-1})
K_a = Reation constant describing affinity (L/mg)
K_F = Reaction constant reflecting ads capacity (L/mg)
A = equil ads constant (L/mg)
b = Temkin isotherm constant relating to heat of ads (J/mol)
R = 8.314 J/molK
T = Absolute temp (K)
n = ads intensity

Kinetics

q_e = ads capacity ($mg.g^{-1}$) at equil
k_1 = pseudo 1st order rate constant (min^{-1})
k_2 = pseudo 2nd order rate constant (g/ mg/min)
t = time (min)
k_2 = second-order rate constant (L/(mg·min))
C_e = conc of solute at equil (mg/L)
C = describes the boundary layer thickness
k_{id} = intra-particle diffusion rate constant ($mg/g/min^{1/2}$)
R^l = Liquid film diffusion constant (min^{-1})
D_e^l = effective liquid film diffusion coefficient (cm^2/min)
r^0 = radius of adsorbent beads (cm)

K′ = ads equil constant

Δr^0 = thickness of liquid film (cm)

Thermodynamics

ΔH = enthalpy change ($Jmol^{-1}$)

ΔS = entropy change ($Jmol^{-1}K^{-1}$)

ΔG = Gibb's free energy change ($Jmol^{-1}$)

R = Molar gas constant (8.314 $Jmol^{-1}K^{-1}$)

T = temperature (K)

K_c =conc equil constant

C_s = conc of analyte on the adsorbent at equil (mgL^{-1})

C_e = conc of analyte in bulk solution at equil (mgL^{-1})

3. Results and Discussion

3.1 Equilibrium Studies

3.1.1 Effect of Initial Concentration

The result of the adsorption of MB onto RDS, TAC, CAC, GT and COM at varying initial dye solution concentrations is presented in Figure 2 (a-b).

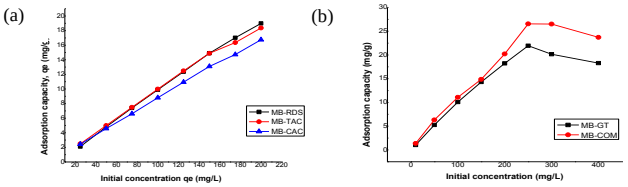

Figure 2: (a) Effect of the initial concentration of MB on RDS, TAC and CAC; (b) Effect of initial concentration of MB on GT and COM

It was shown in Figure 2(a-b) that the adsorption capacity, q_e (mg/g) increased considerably with increasing initial MB concentration for all adsorbents. That of GT and COM increased up to 250 mg/L (optimum concentration) after which the adsorption falls gradually. The initial rise in q_e was due to the high availability of adsorbate ions in solution as MB concentration increases, while the fall in the case of GT and COM may be attributed to saturation of the adsorption sites of the adsorbents at higher concentrations (Gholipour et al., 2011; Li and Zhai, 2020). Amongst the various adsorbents tested, COM exhibited the highest adsorption capacity for MB (23.72 mg/g). Figure 2a further showed that the thermal and chemical treatments in the case of TAC and CAC respectively failed to improve on the adsorption capacity of the date seed adsorbent while the compositing of GT and TAC (Figure 2b) considerably enhanced the adsorption capacity of the constituent adsorbents.

3.1.2 Effect of Initial Solution pH

The initial pH of the dye solution is a significant parameter that controls the adsorption processes. The adsorbent surface charge, degree of ionization of the adsorbate molecule, and the extent of dissociation of functional groups on the active sites of the adsorbent may all be influenced by the pH of the solution (Ramachandran et al., 2011). To observe the effect of pH on the extent of adsorption, therefore, solution pH was varied from 2 – 12 and the results were presented in Table 2 (for RDS, TAC and CAC) and Figure 3 (for GT and COM).

Table 2: Summary of the percentage adsorption for the effect of pH on date seeds (RDS, TAC and CAC).

Effect of pH (% adsorption)			
pH	RDS	TAC	CAC
2	94.40	99.79	90.47
4	98.59	99.85	99.82
6	99.77	99.89	99.82
7	99.79	99.91	99.87
8	99.79	99.91	99.88
10	99.92	99.92	99.92
12	99.93	99.97	99.94

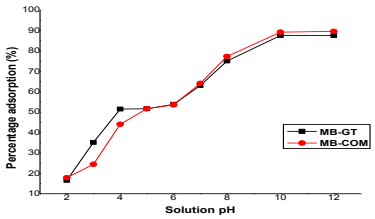

Figure 3: Effect of pH on the sorption of MB onto GT and COM

Table 2 and the curve (Figure 3) showed only a slight influence on the percentage uptake for the date seed adsorbents (RDS, TAC and CAC) and a marked influence with a gradual rise in the uptake for GT and COM as pH increases from 2 to 12, indicating that alkaline medium greatly favours the adsorptive removal of MB. The optimum pH was therefore 12 with the percentage adsorption obtained for the various adsorbents as follows; RDS (99.93%), TAC (99.97%), CAC (99.94%), GT (87.60%) and COM (89.63%). The lower adsorption of MB onto GT and COM at an acidic range of pH was perhaps due to the presence of excess H^+ ions which tend to compete with the dye cations for adsorption sites. At alkaline pH on the other hand, the surface of the adsorbents became negatively charged due to the presence of OH^- ions, which enhances the binding of positively charged dye cations via electrostatic forces of attraction. However, the adsorption of MB onto RDS, TAC and CAC showed over 90% removal even in acidic pH values. This may be that at low pH, MB remains at the cationic and molecular form and can easily penetrate into the pores on the surface of the adsorbent. As the pH increases, the adsorbent surface becomes increasingly negative, making it favourable for the cationic dye adsorption (Hameed et al., 2008). As a result, the sorption of MB onto RDS, TAC and CAC is not only governed by electrostatic interactions but also by van der Waal forces of attraction, π- and other chemical interactions between MB and the adsorbents surfaces (Luo et al., 2019).

3.1.3 Effect of Adsorbent Dosage

The removal of MB at varying adsorbent loads (0.05, 0.1, 0.15, 0.20, 0.25 and 0.5 g) was studied for the influence of adsorbent dosage on the adsorption efficiency. The result is as shown in Figure 4 (a-b).

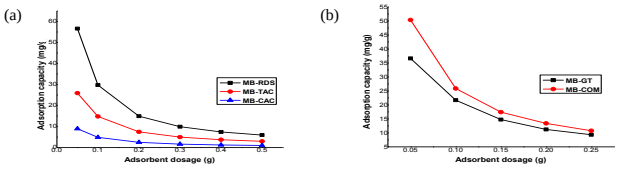

Figure 4: (a) Effect of adsorbent dosage on sorption of MB onto RDS, TAC and CAC; (b) Effect of adsorbent dosage on sorption of MB onto GT and COM

The result of the study showed that with increasing adsorbent load, the amount of MB sorbed onto the unit weight of the adsorbents cuts down as shown by the declining curve of q_e versus adsorbent dose (Figure 4a-b). This may be as a result of the overlapping or aggregation of adsorption sites, leading to a decrease in overall available adsorbent surface area and an increase in diffusion path length (Bahramifar et al., 2015; Gandhimathi et al., 2013).

3.1.4 Effect of Contact Time

Time has a greater influence on the adsorption process as it provides insight into the rate of reaction and the time the adsorption process reaches equilibrium (Gurani, 2015). The effect of time on the adsorption of MB was studied between 5 and 120 minutes at constant optimum concentration and pH. Figures 5a-b illustrate the adsorption of the dye at different time duration.

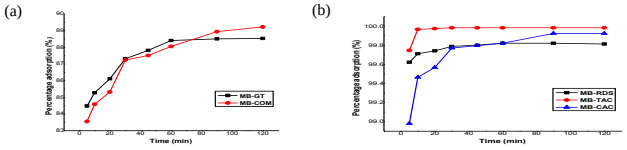

Figure 5: (a) Effect of contact time on sorption of MB onto RDS, TAC and CAC; (b) Effect of contact time on sorption of MB onto GT and COM

The effect of time on adsorption of MB on RDS, TAC and CAC showed rapid uptake within 5 min with 99.622 %, 99.745 % and 98.98 % adsorption respectively as shown in Figure 5a. This may be due to the existence of highly bare and easily accessible surfaces of the adsorbents (Eman et al., 2014). The moment of rapid uptake was followed by minimal incremental adsorption to equilibrium at 60 min for RDS (99.821%), 30 min for TAC (99.983%) and 90 min for CAC (99.924%), after which no further adsorption took place because of the saturation of the active sites on adsorbents surfaces due to prolonged time. This was also observed in the adsorption of binary systems of some basic dyes as reported by (Gandhimathi et al., 2013).

The adsorption of MB onto GT and COM (Figure 5b) followed a similar trend with rapid adsorption during the first 5 min of 84.48% and 83.55% respectively, increasing gradually to 88.54% and 89.22% at 120 minutes. This showed that equilibrium was achieved at the longest time studied, though with very minimal difference in the rate of uptake as the time increases. A similar trend was reported by Kanawade and Gaikwad for adsorption of MB on activated carbon and water hyacinth, Oden and Ozdemr for MB removal using Boron ore and leach waste materials (Kanawade and Gaikwad, 2011; Oden and Ozdemr, 2014).

3.2 Isotherm Study

Equilibrium isotherm study helps in providing insight into the process mechanism, surface properties and affinities of the adsorbents (Dawodu et al., 2012). The relationship between equilibrium concentration and the adsorbate quantity sorbed at constant temperature is defined by the adsorption isotherm. It describes graphically how adsorbates interact or bind with adsorbents using the values of correlation coefficient (R^2) and other parameters to determine the conformity or the suitability of the isotherm model in describing the experimental data (Zargar et al., 2011). The data generated from the variation of concentration experiment were tested for fitness into three common isotherm models; Freundlich, Langmuir and Temkin models. The result of the various isotherm parameters is shown in Table 3 and the best plots presented in Figure 6a-d.

Table 3: Summary of isotherm parameters for the sorption of MB onto RDS, TAC, CAC, GT and COM

Parameters	RDS	TAC	CAC	GT	COM
q_{exp} (mg/g)	18.983	18.365	16.753	21.946	26.561
Langmuir					
R^2	0.104	0.995	0.838	0.942	0.963
q_m (mg/g)	16.666	18.181	23.255	22.72	27.02
K_L (L/mg)	0.244	3.43	0.064	0.02	0.044
R_L (L/mg)	0.026	0.0038	0.382	0.129	0.082
Freundlich					
R^2	0.009	0.484	0.966	0.886	0.948
n	12.345	4.716	1.937	1.464	1.818
1/n	0.081	0.212	0.516	0.683	0.55
K_F (L/mg)	8.465	10.772	2.557	0.715	1.787
Temkin					
R^2	0.121	0.718	0.831	0.869	0.83
A (L/mg)	45.028	346.476	1.45	0.332	0.898
B (J/mol)	2.382	2.129	3.67	4.901	4.837
b_0 (J/mol)	1057.574	1183.251	686.414	514	520.8

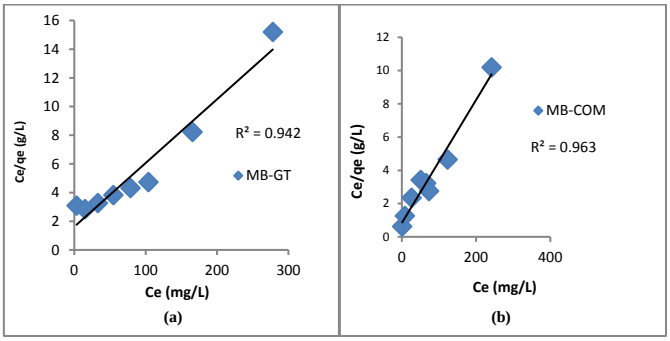

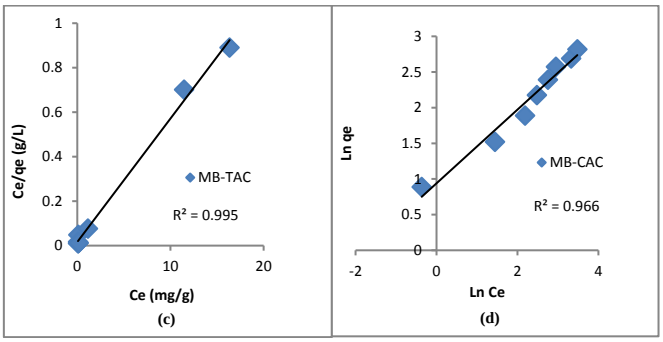

Figure 6: Adsorption isotherm plots (a) Langmuir MB-GT (b) Langmuir MB-COM (c) Langmuir MB-TAC (d) Freundlich MB-CAC

The various values of regression coefficients (R^2) as shown in Table 3 revealed the order of fittings; Langmuir (0.942 and 0.963) > Freundlich (0.886 and 0.948) > Temkin (0.869 and 0.83) for GT and COM respectively. Freundlich model best described the adsorption onto CAC (R^2 = 0.966) while the Langmuir model (R^2 = 0.995) fitted perfectly MB-TAC. MB-RDS showed very poor fittings into the three models with values of R^2 < 0.20. The Langmuir isotherm theory holds for monolayer adsorption onto a homogeneous surface having a finite number of identical sites and assumes the interaction between adsorbed molecules can be negligible (Langmuir, 1916). It equally assumes that after monolayer adsorption, the adsorbent surface becomes saturated (Othamana et al., 2018).

The goodness of fits of Langmuir isotherm into MB-TAC, MB-GT and MB-COM was further confirmed by the closeness of the respective values of monolayer adsorption capacity (q_m) (18.181, 22.72 and 27.02 mg/g) to those obtained experimentally (q_e) (18.365, 21.946 and 26.561mg/g). This is due to the homogenous distribution of the active sites on the surface of the adsorbents (TAC, GT and COM) and thus allowed for monolayer coverage. The data generated from the adsorption experiment were subjected to the equation of separation factor, R_L to ascertain the favourability of the sorption process (Ugbe and Anebi, 2018). For favourable adsorption, $0<R_L<1$, while for unfavourable adsorption, $R_L>1$ and when $R_L = 0$, adsorption is a linear and irreversible process (Dada et al., 2020). The values of the separation factor obtained in all the adsorption systems as shown in Table 3 are less than 1, indicating the favourability of the various processes. Table 4 compares the values of q_m obtained from this study with those of other adsorbents for removal of MB.

Freundlich isotherm model assumes multilayer adsorption, with non-uniform distribution of adsorption heat and affinities over the heterogeneous surface of adsorbents (Freundlich, 1906; Ugbe et al., 2014). The value of n which is a dimensionless constant can depict the type of adsorption process. For n > 1 or n < 1 the adsorption process is by chemosorption or physisorption respectively (Piccin et al., 2011). The good applicability of the Freundlich model to MB-CAC, MB-GT, MB-COM and by extension to MB-TAC indicates multilayer adsorption was involved in the process mechanism. This is in agreement with the results obtained by (Ugbe et al., 2018; Boparai et al., 2010). The values of n all are greater than 1 as seen from Table 3, reflecting a high affinity between the dye and the various adsorbents and indicative of the chemisorptions process (Taha et al., 2009). Thus, the adsorption of MB onto CAC, GT, COM and TAC may proceed by multilayer adsorption on top of the already chemisorbed layer. The Temkin isotherm model assumes that heat of adsorption (a function of temperature) of all molecules in the layer would decrease linearly rather than logarithmically with coverage and corroborates the chemical adsorption process (Foo and Hameed, 2010; Temkin and Pyozhev, 1940). The goodness of fit of Temkin isotherm further supports the findings that the adsorption of MB onto TAC, CAC, GT and COM surfaces may involve a chemisorptions process. This is in agreement with the results obtained by (Shahryari et al., 2010). The Temkin constant (b_0) related to the heat of adsorption which decreases linearly rather than logarithmically as the surface of the adsorbent is loaded due to adsorbent-adsorbate interaction, is in the order; TAC (1183.251 J/mol) > CAC (686.414) > COM (520.8) > GT (514), suggesting a greater interaction between the dye and the various adsorbents in the order; GT > COM > CAC > TAC, which corresponds to decrease in the heat of sorption of all molecules in the layer (Dada et al., 2012).

From the results of the isotherm study, it can be concluded that the adsorption processes of MB onto the TAC, CAC, GT and COM were favourable and probably proceeded by a multilayer physical adsorption on top of the already chemisorbed layer. The tested isotherm models could not describe the adsorption process of MB onto RDS and perhaps the

result of kinetics and thermodynamic studies could hold useful information concerning this.

Table 4: Comparison of monolayer adsorption capacity (q_m) for methylene blue on different adsorbent materials

Adsorbents	q_m (mg/g)	Author (s)
Pumice stone	15.87	(Derakhshan et al., 2013)
Natural Jordanian Tripoli	16.6	(Alzaydien, 2009)
Dry polymer beads	10.638	(Yadav et al., 2020)
KOH treated *Metroxylon spp.*	212.8	(Amode et al., 2016)
Miswak leaves	200	(Elmorsi, 2011)
Magnetic chitosan composite	0.1308	(Jumadi et al., 2019)
Palm branches	14.30	(Eman et al., 2014)
AC of *posidonia oceanica*	175.44	(Elmorsi et al., 2011)
TAC	18.18	This study
GT	22.72	This study
COM	27.02	This study

3.3 Adsorption Kinetics

The study of kinetics in the adsorption process helps to determine the adsorption rate as a function of contact time, which provides information on the process mechanism and that is useful in determining rate-limiting step(s) in the mechanism of the adsorption (Eldin et al., 2016). The closeness to 1 of the correlation coefficient (R^2) values of any kinetic plot indicates the goodness of fit of the applied model (Tsibranska and Hristova, 2011). The data obtained from the effect of time experiment was fitted into common kinetic models; pseudo-first-order, pseudo-second-order, intra-particle diffusion and film diffusion models. The various parameters obtained and best kinetic plots are shown in Table 5 and Figures 7a-f respectively.

Table 5: Summary of adsorption kinetic parameters for sorption of MB onto RDS, TAC, CAC, GT, and COM

Parameters	RDS	TAC	CAC	GT	COM
q_{exp} (mg/g)	14.973	7.499	2.498	33.20	33.45
Pseudo-first order					
R^2	0.364	0.757	0.873	0.978	0.971
K_1 (min^{-1})	0.059	0.2	0.038	0.062	0.034
q_{cal} (mg/g)	0.014	0.025	0.019	2.64	2.6
Pseudo-second order					
R^2	1	1	1	1	1
K_2 (g/mg/min)	0	0	6.153	0.069	0.036
q_{cal} (mg/g)	15.151	7.518	2.5	33.33	34.482
Intra particle diffusion					
R^2	0.734	0.341	0.743	0.872	0.931
Kd	0.003	0.001	0.002	0.182	0.248
C	14.94	7.488	2.477	31.5	30.99
Liquid Film Diffusion					
R^2	0.963	0.757	0.875	0.978	0.970
R'	0.057	0.2	0.038	0.062	0.034

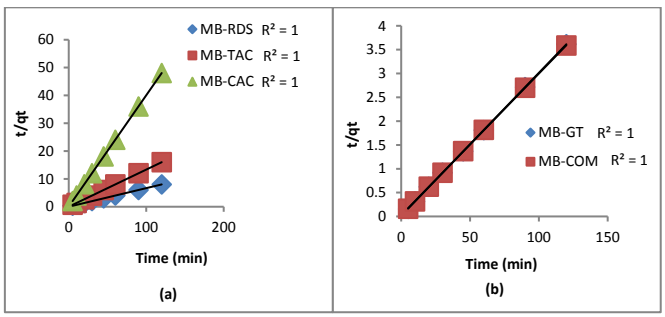

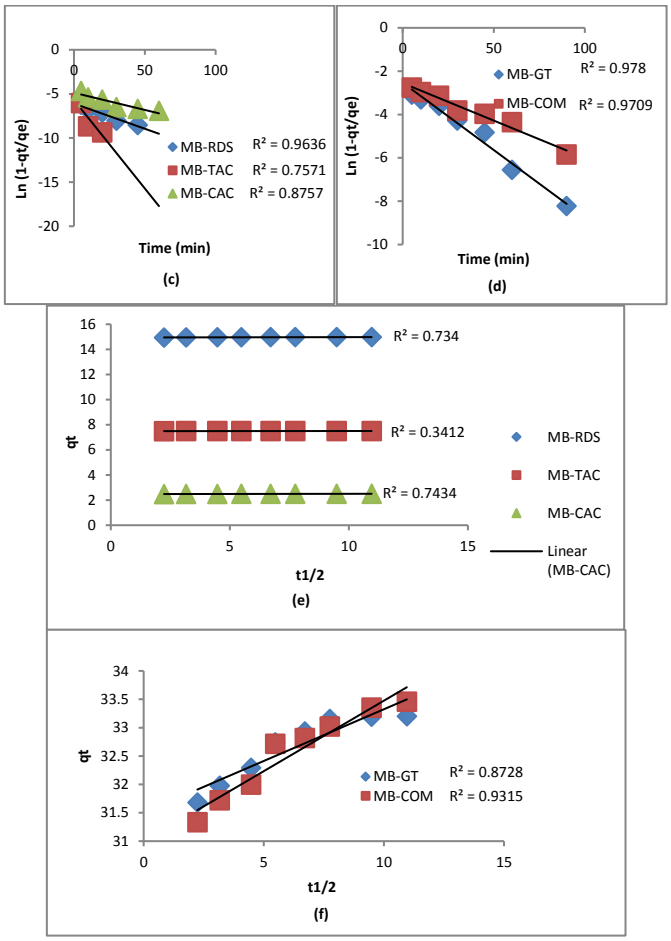

Figure 7: Adsorption kinetic plots (a) Pseudo-second order for RDS, TAC and CAC (b) Pseudo-second order for GT and COM (c) Film diffusion for RDS, TAC and CAC (d) Film diffusion for GT and COM (e) intra-particle diffusion for RDS, TAC and CAC (f) intra-particle diffusion for GT and COM

The adsorption process of MB onto RDS, TAC, CAC, GT and COM as shown in Table 5 fitted pseudo-first-order kinetic model in the order; GT (R^2 =0.978) > COM (0.971) > CAC (0.873) > TAC (0.757) > RDS (0.364). However, the theoretical values of q_e (q_{cal}) were found to be widely different from those obtained experimentally (q_{exp}) for all adsorbents, which showed that the pseudo-first-order kinetic model could not describe the adsorption process of MB onto the various adsorbents. A similar observation was earlier reported by Arladan in the removal of MB onto raw date palm seeds, and other study in the use of bottom ash (an industry waste) for the removal of MB (Ardalan, 2014; Gandhimathi et al., 2013). The pseudo-second-order model is based on the assumption that the rate-determining step may be chemical adsorption involving valence forces through the sharing or exchange of electrons between the adsorbent and the adsorbate.

It is assumed that the sorption capacity is proportional to the number of active sites occupied on the adsorbent (Ho and Mc Kay, 1998; Zulfikar et al., 2013). It was observed from Table 5 and Figure 7a-b that the adsorption of MB onto all the adsorbent fitted perfectly into the pseudo-second-order kinetic model, having all the correlation coefficient (R^2) values to be 1. More so, the values of the theoretically obtained equilibrium sorption capacity, q_{cal} (15.151, 7.518, 2.5, 33.33 and 34.482 mg/g) are in close agreement with those obtained experimentally, q_{exp} (14.973, 7.499, 2.498, 33.20 and 33.45 mg/g) for RDS, TAC, CAC, GT and COM respectively, which further supported the finding that the processes were adequately described by pseudo-second-order model, thus indicating that chemisorption was involved in the mechanism of the adsorption.

This observation was in agreement with the results obtained for some study for the adsorption of MB using Miswak leaves and waste aqua-cultural shell powders respectively (Elmorsi, 2011; Wen-Tien et al., 2009). To effectively ascertain the rate-limiting step in the mechanism of these adsorption processes, the intra-particle diffusion model otherwise known as the Weber-Morris model and the liquid film diffusion model were equally used in the experimental data modeling. Weber-Morris model assumes diffusion into the internal pores of the adsorbents (micropores

and mesopores) while the film diffusion model depicts the movement of the solute molecules from the aqueous phase to the surface of the solid particulates. These steps are being referred to as the mechanism of adsorption and cannot be explained by the kinetics of chemical reactions (Oladoja et al., 2008; Mittal et al., 2007).

The mechanism of the adsorption of MB onto RDS, TAC, CAC, GT and COM was better described by the film diffusion model as shown in Table 5 and Figures 7c-f with the correlation coefficient (R^2) values in the order; GT (0.978) > COM (0.970)> RDS (0.963)> CAC (0.875)> TAC (0.757). This showed that the rate-controlling step in the adsorption processes was the liquid film diffusion mechanism. However, the plots of both models failed to pass through the origin (Figures 7c-f). This signifies that none of the models is the sole rate-limiting step in the adsorption processes or that other processes occurred simultaneously with these two processes in the mechanism of the adsorption (Eldin et al., 2016). In conclusion to the kinetic studies of the adsorption of MB onto RDS, TAC, CAC, GT and COM, the adsorption could involve chemisorption process as suggested by the Pseudo-second order model, and that the mechanism of the adsorption occurred by the two processes (intra-particle and film diffusion) simultaneously as the rate-controlling steps or that other processes occurred simultaneously with these two processes in the mechanism of the adsorption.

3.4 Thermodynamic Study

The effect of temperature on the adsorption of MB on the various adsorbents was investigated at different temperatures (25, 30, 40 and 50 ºC) for RDS, TAC and CAC, and 30, 40, 50, 60, 70 and 80 ºC for GT and COM, to calculate some thermodynamic parameters such as Gibb's free energy change (ΔG), enthalpy change (ΔH) and entropy change (ΔS). The results are shown in Figures 8a-d and Table 6.

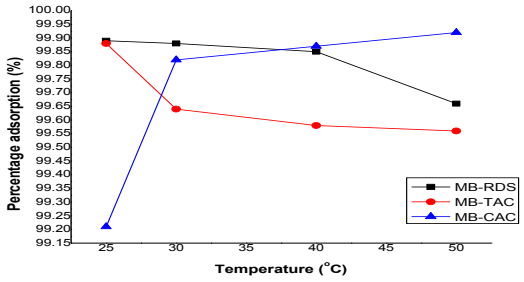

(a)

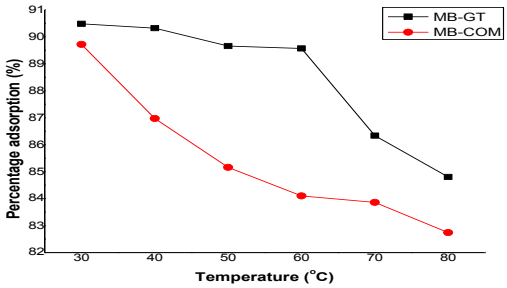

(b)

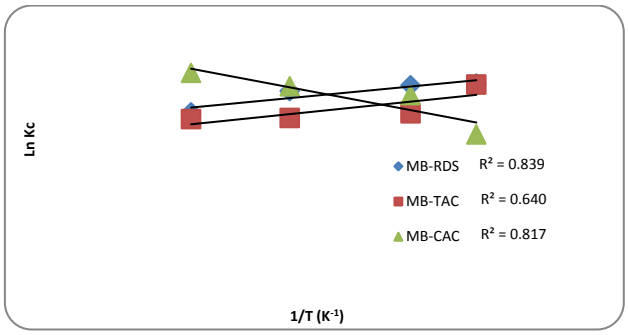

(c)

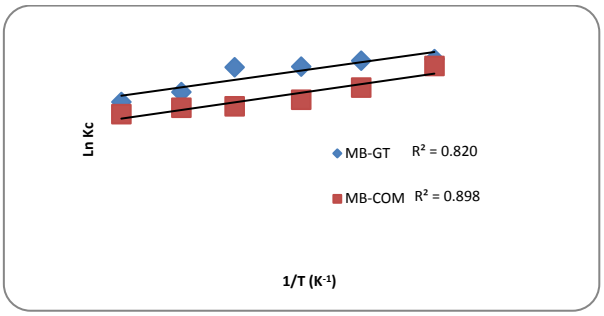

(d)

Figure 8: (a) Effect of temperature on sorption of MB onto RDS, TAC and CAC; (b) Effect of temperature on sorption of MB onto GT and COM; (c) Van't Hoff's plot for sorption of MB onto RDS, TAC and CAC; (d) Van't Hoff's plot for sorption of MB onto GT and COM

Table 6: Summary of the thermodynamic parameters for sorption of MB onto RDS, TAC, CAC, GT and COM

Adsorption Thermodynamics	Parameters				
	T (K)	q_e (mg/g)	ΔG (kJ/mol)	ΔS (kJ/mol .K)	ΔH (kJ/mol)
MB - RDS	298	14.9828	-16.7729	-0.05669	-33.9627
	303	14.9815	-16.8741		
	313	14.9771	-16.8676		
	323	14.9484	-15.2236		
MB - TAC	298	7.4911	-16.6827	-0.06572	-35.2264
	303	7.4732	-14.189		
	313	7.4682	-14.2018		
	323	7.4669	-14.5498		
MB - CAC	298	2.4802	-11.9746	0.262556	65.08199
	303	2.4955	-15.9397		
	313	2.4968	-17.3427		
	323	2.4981	-19.2699		
MB - GT	303	33.9315	-5.67363	-0.01225	-9.60267
	313	33.8694	-5.81121		
	323	33.6210	-5.79938		
	333	33.5876	-5.95241		
	343	32.3752	-5.25652		
	353	31.801	-5.04557		
MB-COM	303	33.6449	-5.45764	-0.01536	-9.86872
	313	32.6131	-4.93951		
	323	31.9347	-4.69182		
	333	31.5382	-4.61195		
	343	31.4484	-4.69968		
	353	31.0271	-4.59958		

The negative values of ΔG reported for all adsorbents (Table 6) suggest the feasibility and spontaneity of the adsorption process for the range of temperature tested. A similar result was reported (Ughe et al., 2014; Muhammad et al., 2014; Boparai et al., 2010). The positive value of ΔS for MB-CAC (Table 6) showed increased randomness at the solid/solution interface. The adsorbed solvent molecules, which were displaced by the adsorbate, gained more translational entropy than is lost by the adsorbate, thus allowing for the prevalence of randomness in the system [70]. An opposite trend was observed for RDS, TAC, GT and COM where ΔS is negative, indicating less randomness at the solid/solution interface. Figures 8a-b showed that the uptake of MB on all adsorbents studied decreased with an increase in temperature (exothermic process) except for that of CAC which followed the opposite trend (endothermic process). This is confirmed by the negative values of ΔH reported in Table 6 for all adsorbents, except for CAC as evident in the slightly enhanced removal at increased temperature. The magnitude of ΔH values for the sorption of MB onto RDS, TAC and CAC fall into the range of 20.9–80 kJ/mol, an indicative of combined physisorption and chemisorptions mechanism at work. Those of GT and COM have enthalpy changes of below 20.9 kJ/mol; indicating physical adsorption process (Saha and Chowdhury, 2011; Muhammad et al., 2014; Ugbe et al., 2014). The deviation of CAC from the other adsorbents in terms of enthalpy and entropy changes may be attributed to the chemical modification of the date palm seed. This is in agreement with those of removal of metal ions using EDTA modified maize cob, chemically modified cassava peel, chemically modified green algal biomass and chemically modified pomelo peel's pulp (Schwantes et al., 2016; Khan et al., 2016; Yang et al., 2019).

4. Conclusion

The results of the study have shown that uptake of MB by the various adsorbents is dependent on the initial solution concentration, pH, adsorbent dosage, contact time and temperature. The experimental data fitted well-tested isotherm models in the order; Langmuir > Freundlich > Temkin for GT and COM while Freundlich and Langmuir models best described the adsorption onto CAC and TAC respectively with RDS showing very poor fittings into the tested isotherms. The adsorption kinetics was best described by pseudo-second-order and film diffusion models, an indication of chemisorptions taking part in the overall process mechanism while the thermodynamics study showed that the processes were feasible, spontaneous and exothermic in nature, except MB-CAC which is endothermic. The combined results of isotherms, kinetics and thermodynamic studies revealed that the adsorption proceeded by a combined physisorption and chemisorption processes. Additionally, the mechanism of the adsorption occurred by the two processes (intra-particle and film diffusion) either simultaneously or that other processes occurred concurrently with these two processes. This study could therefore provide useful information on MB fixation onto date palm seeds, goethite and their composite.

References

Abdullahi, M., Hamza, A.M., Yahaya, S.A., Sanusi, M.K., Sambo, B.E., Abba, S.B., 2015. The potential of establishing date palm (*Phoenix dactylifera L.*) plantation in Sudano-Sahelian Region of Nigeria. Conference: Farm Management Association of Nigeria (FAMAN) held at General Studies Auditorium, Federal University Dutse, Jigawa State, Nigeria.

Abdus-Salam, N., Ikudayisi, V.A., 2017. Preparation and characterization of synthesized goethite and goethite-date palm seeds charcoal composite. Ife Journal of Science, 19 (1), Pp. 99 – 107.

Abdus-Salam, N., Ugbe, F.A., Ikudayisi-Ugbe, A.V., 2020. Optimization and sorption isotherms analysis of anionic dye eosin yellow decontamination by goethite adsorbents. Acta ScientificaMalaysia, 4 (2), Pp. 51-57.

Al-Anber, M.A., 2011. Thermodynamics approach in the adsorption of heavy metals. thermodynamics - interaction studies - solids, liquids and gases, Dr. Juan Carlos Moreno PirajÃ¡n (Ed.), Pp. 738-761.

ALzaydien, A.S., 2009. Adsorption of methylene blue from aqueous solution onto a low-cost natural Jordanian tripoli. American Journal of Environmental Sciences, 5 (3), Pp. 197-208.

Amode, J.O., Santos, J.H., Alam, Z.M., Mirza, A.H., Mei, C.C., 2016. Adsorption of methylene blue from aqueous solution using untreated and treated (*Metroxylon spp.*) waste adsorbent: equilibrium and kinetics studies. Int. J. Ind. Chem., 7, Pp. 333–345.

Anebi, P.O., Ugbe, F.A., Ikudayisi, V.A., 2016. Equilibrium, kinetics and thermodynamic properties of methylene blue adsorption by termite mound. Chem. Soc. Nigeria Conf. Proc.39th Annual Conf., Pp. 57-62.

Anirudhan, T.S., Rejeena, S.R., 2015. Photocatalytic degradation of eosin yellow using poly (pyrrole-co-aniline)-coated TiO2/nanocellulose composite under solar light irradiation. Journal of Materials.

Ansari, R., Mosayebzadeh, Z., 2010. Removal of eosin Y, an anionic dye, from aqueous solutions using conducting electroactive polymers. Iranian Polymer Journal, 19 (7), Pp. 541-555.

Ardalan, J.A., 2014. Removal of methylene blue from aqueous solution using untreated palm seeds powder. Institute of Graduate Studies and Research, Eastern Mediterranean University, Pp. 1-45.

Arshad, I.E., Minerva, E.M., Hisham, A.H., Farouk, M., Abdel, A., 2014. Adsorption of heavy metals from industrial wastewater using palm date pits as low cost adsorbent. International Journal of Engineering and Advanced Technology, 3 (5), Pp. 71-76.

Arunachalam, A., Chaudhuri, R.G., Iype, E., Kumar, B.G.P., 2018. Surface modification of date seeds (Phoenix dactylifera) using potassium hydroxide for wastewater treatment to remove azo dye. Water Practice and Technology, 13 (4), Pp. 860 – 870.

Bahramifar, N., Tavasolli, M., Younesi, H., 2015. Removal of eosin Y and eosin B dyes from polluted water through biosorption using *Saccharomyces cerevisiae*: Isotherm, kinetic and thermodynamic studies, Journal of Applied Research in Water and Wastewater, 3, Pp. 108-114.

Boparai, H.K., Joseph, M., O'Carroll, D.M., 2010. Kinetics and thermodynamics of cadmium ion removal by adsorption onto nano zerovalent iron particles. Journal of Hazardous Materials, Pp. 1-8.

Borah, L., Goswami, M., Phukan, P., 2015. Adsorption of methylene blue and eosin yellow using porous carbon prepared from tea waste: Adsorption equilibrium, kinetics and thermodynamics study. Journal of Environmental Chemical Engineering, 565, Pp. 1–11.

Boyd, G.E., Adamson, A.W., Meyers, L.S., 1947. The exchange adsorption of ions from aqueous solution by organic zeolites II Kinetics. Journal of American Chemical Society, 69, Pp. 2836 –2848.

Chandrasekaran, M., Bahkali, A.H., 2012. Valorization of date palm (Phoenix dactylifera) fruit processing by-products and wastes using bioprocess technology – Review. Saudi Journal of Biological Sciences, 20, Pp. 105–120.

Dada, A.O., Adekola, F.A., Odebunmi, E.O., Dada, F.E., Bello, O.M., Akinyemi, B.A., Bello, O.S., Umukoro, O.G., 2020. Sustainable and low-cost *Ocimum gratissimum* for biosorption of indigo carmine dye: kinetics, isotherm, and thermodynamic studies. International Journal of Phytoremediation, Pp. 1-14.

Dada, A.O., Olalekan, A.P., Olatunya, A.M., Dada, O., 2012. Langmuir, Freundlich, Temkin and Dubinin–Radushkevich isotherms studies of equilibrium sorption of zn^{2+} unto phosphoric acid modified rice husk. IOSR Journal of Applied Chemistry, 3 (1), Pp. 38-45.

Dawodu, F.A., Akpomie, G.K., Ejikeme, P.C.N., 2012. Equilibrium, thermodynamic and kinetic studies on the adsorption of lead(ii) from solution by "agbani clay". Research Journal of Engineering Sciences, 1 (6), Pp. 9-17.

Derakhshan, Z., Baghapour, M.A., Ranjbar, M., Faramarzian, M., 2013. Adsorption of methylene blue dye from aqueous solutions by modified pumice stone: kinetics and equilibrium studies. Health Scope, 2 (3), Pp. 136–144.

El Marouani, M., Azoulay, K., Bencheikh, I., El Fakir, L., Rghioui, L., El Hajji, A., Sebbahi, S., El Hajjaji, S., Kifani-Sahban, F., 2018. Application of raw and roasted date seeds for dyes removal from aqueous solution. J. Mater. Environ. Sci., 9 (8), Pp. 2387-2396.

Eldin, M.S., Aly, K.M., Khan, Z.A., Mekky, A.M., Saleh, T.S., Al- Bogami, A.S., 2016. Removal of methylene blue from synthetic aqueous solutions with novel phosphoric acid-doped pyrazole-g-poly (glycidyl methacrylate) particles: kinetic and equilibrium studies, Desalination and Water Treatment, Pp. 1–16.

Elmorsi, R.R., El-Wakeel, S.T., El-Dein, W.A.S., Lotfy, H.R., Rashwan, W.E., Nagah, M., Shaaban, S.A., Ahmed, S.A.S., El-Sherif, I.Y., Abou-El-Sherbini, K.S., 2019. Adsorption of methylene blue and Pb^{2+} by using acid-activated Posidonia oceanica waste. Scientific Reports, 9, Pp. 3356.

Elmorsi, T.M., 2011. Equilibrium isotherms and kinetic studies of removal of methylene blue dye by adsorption onto miswak leaves as a natural adsorbent. Journal of Environmental Protection, 2, Pp. 817-827.

Eman, A.A., Maha, A.T., Patrick, J.P., 2014. Use of agriculture-based waste for basic dye sorption from aqueous solution: kinetics and isotherm studies. American Journal of Chemical Engineering, 2 (6), Pp. 92-98.

Foo, K.Y., Hameed, B.H., 2010. Insights into the modeling of adsorption isotherm systems (A review). Chemical Engineering Journal, 156, Pp. 2–10.

Freundlich, H.M.F., 1906. Over the adsorption in solution. Journal of Physical Chemistry, 57, Pp. 385–471.

Funtua, M.A., Ugbe, F.A., 2015. Adsorption of heavy metals from aqueous

wastewater using unmodified and ethylenediaminetetraacetic acid (EDTA) modified maize cobs. International Journal of Current Research in Biosciences and Plant Biology, 2 (1), Pp. 98 – 103.

Gandhimathi, R., Ramesh, S.T., Sindhu, V., Nidheesh, P.V., 2013. Bottom ash adsorption of basic dyes from their binary aqueous solutions. Songklanakarin Journal of Science and Technology, 35 (3), Pp. 339-347.

Gholipour, M., Hassan, H., Maryam, M., 2011. Hexavalent chromium removal from aqueous solution via adsorption on granular activated carbon: adsorption, desorption, modeling and simulation studies. Asian Research Publishing Network, 6 (9), Pp. 10-18.

Gurani, K.B., 2015. Adsorption on fluoride removal by using Batch Techniques. Indian Journal Science Resolution, 12 (1), Pp. 209-213.

Hameed, B.H., Mahmoud, D.K., Ahmad, A.L., 2008. Equilibrium modeling and kinetic studies on the adsorption of basic dye by a low-cost adsorbent: Coconut (*Cocos nucifera*) bunch waste. Journal of Hazardous Materials, 158, Pp. 65–72.

Ho, Y.S., McKay, G., 1998. A Comparison of chemisorptions kinetic models applied to pollutant removal on various sorbents. Process Safety and Environmental Protection, 76 (4), Pp. 332 – 340.

Ho, Y.S., McKay, G., 1999. Pseudo second-order model for sorption processes. Process Biochemistry, 34, Pp. 451–465.

Jumadi, J., Kamari, A., Rahim, N.A., Wong, S.T.S., Yusoff, S.N.M., Ishak, S., Ishak, M.M., Kumaran, S., 2019. Removal of methylene blue and congo red by magnetic chitosan nanocomposite: Characterization and adsorption studies. J. Phys.: Conf. Ser., 1397, Pp. 012027.

Kanawade, S.M., Gaikwad, R.W., 2011. Removal of methylene blue from effluent by using activated carbon and water hyacinth as adsorbent. International Journal of Chemical Engineering and Applications, 2 (5).

Khan, T.A., Mukhlif, A.A., Khan, E.A., Sharma, D.K., 2016. Isotherm and kinetics modeling of Pb (II) and Cd (II) adsorptive uptake from aqueous solution by chemically modified green algal biomass, Model. Earth Syst. Environ., 2 (117).

Ladan, M., Ayuba, A.M., Bishir, U., Jamilu, A., and Habibu, S., 2013. Thermodynamic properties of chromium adsorption by sediments of River Watari, Kano State. Chemsearch Journal, 4, Pp. 1 – 5.

Lagergren, S., 1998. About the theory of so-called adsorption of soluble substances. Kungliga Svenska Vetenskapsakademiens Handlingar, 24 (4), Pp. 1-39.

Langmuir, I., 1916. The constitution and fundamental properties of solids and liquids. Journal of American Chemical Society, 38 (2629), Pp. 25.

Li, X., Zhai, Q., 2020. Evaluation of eosin Y removal from aqueous solution using nano‐mesoporous material MCFs: adsorption equilibrium, kinetics, and adsorption isotherms, International Journal of Industrial Chemistry; https://doi.org/10.1007/s40090-020-00202-4.

Liu, H., Chen, T., Frost, R.L., 2013. An overview of the role of goethite surfaces in the environment, Chemosphere, xxx, xxx-xxx.

Luo, L., Wu, X., Li, Z., Zhou, Y., Chen, T., Fan, M., and Zhao, W., 2019. Synthesis of activated carbon from biowaste of fir bark for methylene blue removal. R. Soc. open sci., 6, Pp. 190523.

Mittal, A., Lisha, K., Jyoti, M., 2007. Freundlich and Langmuir adsorption isotherms and kinetics for the removal of tartrazine from aqueous solutions using hen feathers. Journal of Hazardous Materials, 146, Pp. 243–248.

Mohamed, A.H., Ahmed, E., 2017. Health and environmental impacts of dyes: Mini-Review. American Journal of Environmental Science and Engineering, 1 (3), Pp. 64-67.

Muhammad, A.A., Audu, U.F., Pam, A.A., Onakpa, S.A., 2014. Thermodynamic study of the competitive adsorption of chromium (iii) ions and halides onto sweet orange (*citrus sinensis*) peels as adsorbent. J. Environ Anal Chem., 1 (2).

Nayak, R., and Rao, J.R., 2005. Synthesis of active goethite and maghemite from scrap iron sources. Journal of scientific and industrial research, 64, Pp. 35 – 40.

Oden, M.K., Ozdemr, C., 2014. Removal of methylene blue dye from aqueous solution using natural boron ore and leach waste material: adsorption optimization criteria. International Journal of Current Research and Academic Review, 1, Pp. 66-71.

Oladoja, N.A., Aboluwoye, C.O., Oladimeji, Y.B., 2008. Kinetics and isotherm studies on methylene blue adsorption onto ground palm kernel coat. Turkish Journal of Engineering and Environmental Science, 32, Pp. 303 – 312.

Othmana, N.H., Aliasa, N.H., Shahruddina, M.Z., Bakara, N.F.A., Hima, N.R.N., Laub, W.J., 2018. Adsorption kinetics of methylene blue dyes onto magnetic graphene oxide. Journal of Environmental Chemical Engineering, 6, Pp. 2803–2811.

Piccin, J.S., Dotto, G.L., Pinto, J.L.A., 2011. Adsorption isotherms and thermochemical data of FD & C red N° 40 binding by chitosan. Brazilian Journal of Chemical Engineering, 28 (02), Pp. 295 – 304.

Ramachandran, P., Vairamuthu, R., Ponnusamy, S., 2011. Adsorption isotherms, kinetics, thermodynamics and desorption studies of reactive orange 16 on activated carbon derived from ananas comosus (L.) carbon. Journal of Engineering and Applied Sciences, 6 (11), Pp. 15-26.

Saha, P., Chowdhury, S., 2011. Insight into adsorption thermodynamics. InTech, 16, Pp. 350-364.

Saini, R.D., 2017. Textile organic dyes: polluting effects and elimination methods from textile wastewater. International Journal of Chemical Engineering Research, 9 (1), Pp. 121-136.

Sajab, M.S., Chia, C.H., Zakaria, S., Jani, S.M., Ayob, M.K., Chee, K.L., Khiew, P.S., Chiu, W.S., 2011. Citric acid-modified kenaf core fibres for removal of methylene blue from aqueous solution. Bioresource Technology, 102 (15), Pp. 7237-7243.

Schwantes, D., GonçalvesJr, A.C., Coelho, G.F., Campagnolo, M.A., Dragunski, D.C., Tarley, C.R.T., Miola, A.J., Leismann, E.A., 2016. Chemical modifications of cassava peel as adsorbent material for metals ions from wastewater. Journal of Chemistry, http://dx.doi.org/10.1155/2016/3694174.

Shahryari, Z., Goharrizi, A.S., Azadi, M., 2010. Experimental study of methylene blue adsorption from aqueous solutions onto carbon nanotubes. International Journal of Water Resources and Environmental Engineering, 2 (2), Pp. 016-028.

Taha, M.R., Ahmad, K., Aziz, A.A., Chik, Z., 2009. Geo-environmental aspects of tropical residual soils. In: Huat, B.B.K., Sew, G.S. and Ali, F.H., Eds. Tropical Residual Soils Engineering, A.A. Balkema Publishers, London, Pp. 377-403.

Temkin, M.I., Pyozhev, V., 1940. Kinetics of ammonia synthesis on the promoted iron catalyst. Acta Phys. Chim. USSR, 12, Pp. 327–356.

Tsibranska, I., Hristova, E., 2011. Comparison of different kinetic models for adsorption of heavy metals onto activated carbon from apricot stones. Bulgarian Chemical Communications, 43 (3), Pp. 370 – 377.

Ugbe, F.A., Abdus-Salam, N., 2020. Kinetics and thermodynamic modeling of natural and synthetic goethite for dyes scavenging from aqueous systems. Arab. J. Chem. Environ Res., 7 (1), Pp. 12-28.

Ugbe, F.A., Anebi, P.O., Ikudayisi-Ugbe, A.V., 2018. Biosorption of an anionic dye, eosin yellow onto pineapple peels: isotherm and thermodynamic study. International Annals of Science, 4 (1), Pp. 14-19.

Ugbe, F.A., Pam, A.A., Ikudayisi, A.V., 2014. Thermodynamic properties of chromium (III) ion adsorption by sweet orange (*citrus Sinensis*) peels. American Journal of Analytical Chemistry, 4 (5), Pp. 666-673.

Utsev, J.T., Iwar, R.T., Ifyalem, K.J., 2020. Adsorption of methylene blue from aqueous solution onto delonix regia pod activated carbon: batch equilibrium isotherm, kinetic and thermodynamic studies. J. Mater. Environ. Sci., 11 (7), Pp. 1058-1078.

Wang, X., Chen, N., Zhang, L., 2019. Enhanced Cr (VI) immobilization on goethite derived from an extremely acidic environment. Environ. Sci. Nano., 6, Pp. 2185 – 2194.

Weber, W.J., Morris, J.C., 1963. Kinetics of adsorption on carbon from solutions, Journal of Sanitation Division. American Society of Civil Engineering, 89, Pp. 319.

Wen-Tien, T., Chen, H.R., Kuo, K.C., Lai, C.Y., Su, T.C., Chang, Y.M., Yang, J.M., 2009. The Adsorption of methylene blue from aqueous solution using waste aquacultural shell powders. Journal of Environmental and Engineering Management, 19 (3), Pp. 165-172.

Yadav, S., Asthana, A., Chakraborty, R., Jain, B., Singh, A.K., Carabineiro, S.A.C., Susan, A.H., 2020. Cationic dye removal using novel magnetic/activated charcoal/βcyclodextrin/alginate polymer nanocomposite, Nanomaterials, 10, Pp. 170.

Yang, P., Xu, Y., Tuo, J., Li, A., Liu, L., Shi, H., 2019. Preparation of modified pomelo peel's pulp adsorbent and its adsorption to Uranyl ions. R. Soc Open Sci., 6 (3).

Zargar, B., Parham, H., Rezazade, M., 2011. Fast removal and recovery of methylene blue by activated carbon modified with magnetic iron oxide nanoparticles. Journal of the Chinese Chemical Society, 58, Pp. 694-699.

Zhanga, P., Connora, D., Wang, Y., Jiang, L., Xiab, T., Wanga, L., Tsangc, D.C.W., Okd, Y.S., and Houa, D., 2020. A green biochar/iron oxide composite for methylene blue removal. Journal of Hazardous Materials, 384, Pp. 121286.

Zulfikar, M.A., Setiyanto, H., Djajanti, S.D., 2013. Effect of temperature and kinetic modeling of lignosulfonate adsorption onto powdered eggshell in batch systems. Songklanakarin Journalof Science and Technology, 35 (3), Pp. 309 – 16.